approximation of the energy deposited by each individual proton in each layer.
A tracking algorithm is able to find the water equivalent path length of each individual proton. When this information is combined with the approximated energy deposition on each layer, an estimate of the incoming proton energy is obtained by locating the high energy deposit of the Bragg Peak.
Results from this analysis, as well as the capabilities of alternative setups will be presented, to show the feasibility of using such a calorimeter for proton Computed Tomography.

This project is supported by Helse Vest PhD grant 911933.

Keywords: Calorimeter, Hadron Therapy, Pixel Sensors

References:
[1] T. Peitzmann, *Prototype studies for a forward EM calorimeter in ALICE, Proceedings of CHEF2013*, preprint arXiv:1308.2585.
[2] D. Fehlker *et al*. *Electronics for a highly segmented electromagnetic Calorimeter prototype.* TWEPP 2012; 2012-09-17 - 2012-09-21.
[3] S. Jan *et al*., *GATE: a simulation toolkit for PET and SPECT*. Phys. Med. Biol. 49 4543 (2004).

174
Proton Minibeam Radiation Therapy (pMBRT): implementation at a clinical center
C. Peucelle[1], C. Nauraye[2], A. Patriarca[2], L. de Marzi[2], E. Hierso[2], N. Fournier-Bidoz[2],
I. Martínez-Rovira[1] and Y. Prezado[1]
[1] IMNC – UMR 8165, IN2P3-CNRS, Université Paris 7, Université Paris 11, Orsay, France
[2] Institut Curie – Centre de Protonthérapie d'Orsay (ICPO), Orsay, France

Purpose: The more selective energy deposition of protons in depth is advantageous compared to photons to preserve normal tissues. Nevertheless, an even better tissue sparing might be possible in proton therapy if combined with the well-established tissue preservation of spatially fractionated submillimetric beams. This sparing effect has been observed in studies performed with synchrotron minibeam radiotherapy (MBRT) [1,2].
The innovative approach proposed here, called proton minbeam radiation therapy (pMBRT), was shown to lead to favorable dose distributions in Monte Carlo (MC) studies [3]. The dose profiles in normal tissue consist in peaks and valleys, while the tumour receives a (quasi)-homogenous dose distribution [3]. The goal of this study was to implement this promising approach at a clinical center, as well as to gather a complete set of dosimetric data that will serve to guide the ongoing biological experiments [4].
Material and Methods: The implementation of pMBRT was carried out at the Proton Therapy Center in Orsay (ICPO). 100 MeV-proton minibeams (400 and 700 µm-width) were generated by means of a multislit collimator. The dose distributions (depth dose curves, lateral profiles, peak-to-valley dose ratios (PVDR) [6], beam widths and output factors) were measured by means of Gafchromic EBT3 films and the new PTW microDiamond detector [5].
In parallel, a very first MC-based calculation engine for pMBRT is under development using Gate v7.0.
Results: The experimental data confirm that a spatial fractionation of the dose is maintained in normal tissues (PVDR up to 7) while a quasi-homogeneous dose distribution is reached at the Bragg peak location, in agreement with theoretical predictions [3]. The reduced penumbras (600-1100 µm) in healthy tissue make pMBRT a good candidate for radiosurgery applications.
Similar results were obtained using either EBT3 films or the PTW microDiamond detector. The preliminary MC calculations were consistent with experimental dose distributions.
Conclusion: This is the first work providing both a complete set of dosimetric data in such small proton field sizes and a practical implementation of this promising approach using a clinical set-up and beam energy. The dose distributions showed the potential of this technique, which might lead to a reduction of the normal tissue complication probability. Animal irradiation experiments are ongoing to confirm the normal tissue sparing capability of pMBRT.

Keywords: Proton Minibeam Radiation Therapy (pMBRT), small field dosimetry, novel approaches

References:
[1] P. *Deman et al.*, Int. J. Radiat. Oncol. Biol. Phys., 82 (2012)
[2] *Y. Prezado et al.*, Rad. Research 2015
[3] *Y. Prezado et al.*, Med. Phys. 40 (3) (2013).
[4] *C. Peucelle et al.*, *submitted, Med. Phys.*
[5] PTW website (www.ptw.de), microDiamond – Synthetic Diamond Detector Specifications
[6] *F. A. Dilmanian et al., J. Neuro-Oncol. 4, (2002).*

175
Contribution of direct and bystander effects to therapeutic efficacy of alpha-RIT using ^{212}Pb-labeled mAbs
R. Ladjohounlou[1,2,3,4], A. Pichard[1,2,3,4], V. Boudousq[1,2,3,4], S. Paillas[1,2,3,4], M. Le Blay[1,2,3,4], C. Lozza[1,2,3,4], S. Marcatili[5], M. Bardiès[5], J. Torgue[7], I. Navarro-Teulon[1,2,3,4] and J-P Pouget[1,2,3,4]
[1] IRCM, Institut de Recherche en Cancérologie de Montpellier, Montpellier, F-34298, France
[2] INSERM, U1194, Montpellier, F-34298, France
[3] Université de Montpellier, Montpellier, F-34090, France
[4] Institut régional du Cancer de Montpellier, Montpellier, F-34298, France
[5] UMR 1037 INSERM/UPS, Centre de Recherche en Cancérologie de Toulouse, Toulouse F-31062, France
[7] AREVA Med, 4800 Hampden lane, Bethesda, MD 20814, USA

Purpose: We assessed *in vitro* and *in vivo* the relative contribution of direct and bystander effects in the therapeutic efficacy of RIT using ^{212}Pb-labeled mAbs for treating cancer cells.
Materials and Methods: A-431 cells were *in vitro* exposed to increasing activities (0–0.5 MBq/mL; 37 MBq/mg) of either 35A7 (anti-CEA), Trastuzumab (anti-HER2) or PX (non-specific) ^{212}Pb-labeled mAbs. The relative contribution of direct and bystander effects was determined using standard medium transfer protocol. Biological end points included clonogenic survival and DNA double strand breaks (using 53BP1 and gamma-H2AX immunofluorescence detection) measured both in donor (direct effect) and in recipient cells (bystander effects). *In vivo*, nude mice with intraperitoneal (i.p.) 2-3 mm A-431 tumour cells xenografts were i.p. injected with increasing activities (370–1480 kBq; 37 MBq/mg) of the above mentioned anti-CEA, anti-HER2 or non-specific ^{212}Pb-mAbs. Tumour growth was determined and the distribution of radioactivity at the tissue level was assessed using digital micro-autoradiography (DAR) followed by voxel dosimetry. Biological markers including 53BP1 and Ki67 proteins together with abnormal mitosis were also determined on tumour sections.
Results: *In vitro* we showed in donor cells the strong efficacy of ^{212}Pb-35A7 and ^{212}Pb-trastuzumab mAbs and also to a lower extent of ^{212}Pb-PX mAb. Significant bystander cytotoxicity was measured in all recipient cells with the three radiolabeled mAbs. The complexity of DNA damage (53BP1 foci) observed in donor cells confirmed the high LET cytotoxic effects of ^{212}Pb-mAbs while less complex damage were observed in recipient cells.
In vivo DAR and voxel dosimetry indicated the strong heterogeneity in anti-CEA ^{212}Pb-mAbs distribution in tumours. Conversely, distribution of anti-HER2 ^{212}Pb-mAbs was much more homogeneous. These data could explain the lower therapeutic efficacy of the latter mAbs compared with anti-HER2 ^{212}Pb-mAbs (median survival of 94 days for anti-CEA ^{212}Pb-mAbs versus 20 days for control, not reached for anti-HER2 ^{212}Pb-mAbs). Moreover, voxel dosimetry indicated that about 30% of the tumours of mice treated with anti-CEA ^{212}Pb-mAbs received 0Gy. However, we also observed in the same tumours, homogeneous formation of DNA damage

independently of absorbed doses distribution, together with abnormal mitosis. The latter results indicate that bystander effects could also be involved. However, at this stage, we may assume that they do not fully counterbalance the lack of efficacy due to heterogeneous distribution of anti-CEA ^{212}Pb-mAbs, possibly because lesions are not as complex as those produced by high LET radiation.
Conclusions: Our results showed *in vitro* and *in vivo* that, besides the strong direct effect of ^{212}Pb-labeled mAbs in killing tumour cells, bystander effects have also to be considered.

Keywords: Radionuclide therapy, Radiobiology, Bystander effects

176
Predictive Biomarkers for Improving Radiation Therapy
P. Prasanna
Radiation Research Program
National Cancer Institute, National Institute of Health, Bethesda, MD, USA.
Pat.Prasanna@nih.gov

Radiotherapy is an important treatment modality for millions of patients with cancer worldwide. Current treatment decisions do not take into account individual patients' or cohorts of patients' sensitivities to this treatment modality. As such, patients treated with radiation therapy experience a large variation in normal tissue toxicity that results in dose-limiting acute and irreversible progressive side effects. Important examples of these adverse effects include mucositis, pneumonitis, and cognitive damage, respectively representing acute, intermediate, and late effects. Stratification of patients based on radiation sensitivities will allow delivery of suitable alternative treatments to high-risk patients and dose escalation to tumors in less sensitive patients. Current focus on radiation biomarkers/biodosimeters appears to be primarily to assess radiation doses after catastrophic accidental radiation exposure. Recent advances have brought together several cross-disciplinary areas such as biological assays, analytical platforms, and algorithms to rapidly assess dose to individuals. These technologies are at different maturation levels. This immense progress is also an opportunity to use them to predict heterogeneity of radiation sensitivities among cancer patients to improve radiation therapy outcome and their quality of life. This talk will emphasize the need for discovery, development, and validation of predictive biomarkers, provide some examples of biomarkers, and discuss the translational challenges involved in leveraging advances in radiation-specific biomarker research to radiotherapy, which for the foreseeable future likely to remain a cornerstone of cancer treatment.

Disclaimer: Author declares no conflict of interest. Views expressed here are the personal views of the author and does not represent the views of NCI.

177
Prompt gamma imaging of passively shaped proton fields with a knife-edge slit camera
M. Priegnitz*[1], S. Barczyk*[2,3], I. Keitz[2], S. Mein[2], F. V. Stappen[6], G. Janssens[6], L. Hotoiu[6], J. Smeets[6], F. Fiedler[1], D. Prieels[6], W. Enghardt[2-5], G. Pausch[2], C. Richter[2-5]
[1] Helmholtz-Zentrum Dresden – Rossendorf, Institute of Radiation Physics, Bautzner Straße 400, 01328 Dresden, Germany
[2] OncoRay – National Center for Radiation Research in Oncology, Faculty of Medicine and University Hospital Carl Gustav Carus, Technische Universität Dresden, Helmholtz-Zentrum Dresden-Rossendorf, Dresden, Germany
[3] Department of Radiation Oncology, University Hospital Carl Gustav Carus, Technische Universität Dresden, Dresden, Germany
[4] Helmholtz-Zentrum Dresden – Rossendorf, Institute of Radiooncology, Bautzner Straße 400, 01328 Dresden, Germany
[5] German Cancer Consortium (DKTK), Dresden, Germany and German Cancer Research Center (DKFZ), Heidelberg, Germany
[6] Ion Beam Applications SA, Chemin du Cyclotron 3, 1348 Louvain-la-Neuve, Belgium
* Both authors contributed equally to this work

Purpose: Range verification in proton therapy is highly desirable to fully exploit the advantageous properties of proton beams for tumor therapy. In this context, prompt gamma imaging (PGI) is of growing interest and different technical concepts for realization are currently under investigation. The feasibility of range shift detection with a slit camera has previously been shown for different targets irradiated with protons in pencil beam scanning mode [1-3]. In preparation of the clinical application of the slit camera within a patient study, we report on the first application of the slit camera to passively shaped proton beams.
Materials / Methods: Targets with increasing complexity have been irradiated with passively shaped proton beams (double scattering mode). For artificial range shift induction, the energy of the protons was varied. Prompt gamma emission was monitored by means of a knife-edge shaped slit camera.
Prompt gamma rays emitted during the irradiation are projected through a slit aperture onto a segmented detector. Thus, a one-dimensional depth distribution of detected prompt gamma rays is obtained.
In double scattering mode, a high neutron induced background hampers direct range shift evaluation from these detected gamma distributions. In order to quantify this background, measurements have been repeated with a closed slit aperture of the camera. This facilitates a subtraction of the background from the measurements with open slit.
Time resolved analysis of the measurements allows for a mapping of single prompt gamma profiles to different steps of the range modulator wheel, and, thus, to different iso-energy layers.
Results: Global range shifts of several millimeters in homogeneous as well as inhomogeneous targets were detected with the slit camera measurement during proton irradiation with passive field formation. Figure 1 shows the experimental setup with a head target (left) and detected prompt gamma profiles for different proton energies, i.e. different requested proton ranges (right). Separation of different prompt gamma profiles related to single steps of the range modulator wheel was possible.

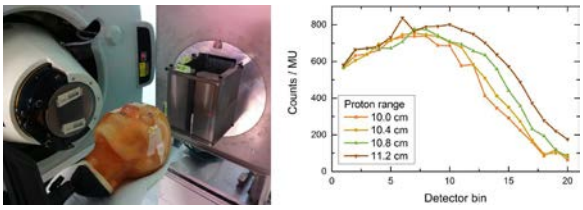

Figure 1: Left: Experimental setup of a prompt gamma slit camera measurement during irradiation of a head phantom with a passively shaped proton beam. Right: Measured prompt gamma depth profiles, normalized to the applied monitor units (MU) for different requested proton ranges, i.e. different proton energies.

Conclusions: In preparation of the application of the slit camera to patient treatment, we investigated the detectability of range shifts in double scattering proton irradiation. Global range shifts of a few millimeters were detected from measurements with the slit camera. Time resolved analysis allows for separation of prompt gamma profiles correlated to protons of different iso-energy layers. This might provide additional information on potential sources of range deviations.

Keywords: prompt gamma imaging, slit camera, proton range verification

References: